

## COMMUNICATION

**Direct Visualization of Substitutional Li Doping in Supported Pt Nanoparticles and Their Ultra-selective Catalytic Hydrogenation Performance**

Tianyi Chen<sup>a,b</sup>, Christopher Foo<sup>a</sup>, Jianwei Zheng<sup>a</sup>, Huihuang Fang<sup>a</sup>, Peter Nellist<sup>b\*</sup> and Shik Chi Edman Tsang<sup>a\*</sup>

<sup>a</sup>Dr Tianyi Chen, Christopher Foo, Dr. J. W. Zheng, Huihuang Fang, Prof. S. C. E. Tsang  
Wolfson Catalysis Centre, Department of Chemistry University of Oxford, Oxford, OX1  
3QR, UK

E-mail: [edman.tsang@chem.ox.ac.uk](mailto:edman.tsang@chem.ox.ac.uk); [peter.nellist@materials.ox.ac.uk](mailto:peter.nellist@materials.ox.ac.uk)

[Twitter: Tsang Group @scetsang](#)

<sup>b</sup>Dr. Tianyi Chen, Prof. Peter Nellist

Department of Materials, University of Oxford, Oxford, OX1 PH, UK

**Abstract:**

It has only recently been established that doping light elements (lithium, boron, and carbon) into supported transition metals can fill interstitial sites, which can be observed by the expanded unit cell. As an example, interstitial lithium (<sup>int</sup>Li) can block H filling octahedral interstices of palladium metal lattice, which improves partial hydrogenation of alkynes to alkenes under hydrogen. In contrast, herein, we report <sup>int</sup>Li is not found in the case of Pt/C. Instead, we observe for the first time a direct ‘substitution’ of Pt with substitutional lithium (<sup>sub</sup>Li) in alternating atomic columns using scanning transmission electron microscopy-annular dark field (STEM-ADF). This ordered substitutional doping results in a contraction of the unit cell as shown by high-quality synchrotron X-ray diffraction (SXRD). The electron donation of d-band of Pt without higher orbital hybridizations by <sup>sub</sup>Li offers an alternative way for ultra-selectivity in catalytic hydrogenation of carbonyl compounds by suppressing the facile CO bond breakage that would form alcohols.

Supported Pd and Pt metal nanoparticles are the central focus for catalytic hydrogenation because both metals have the ability to activate hydrogen under mild conditions.<sup>[1]</sup> Pd can react with hydrogen to form the interstitial hydride PdH<sub>0.7</sub>, which is stable under ambient conditions. Pt is a good hydrogenation catalyst, but does not seem to form stable interstitial hydrides.<sup>[2]</sup> Even though the catalytic properties of these active metal hosts can be significantly enhanced by light-element doping, more details with particular regard to the structure-activity relationships are required. It has only recently been confirmed that apart from hydrogen, some light elements are also able to occupy the same interstitial sites of Pd. For example, carbon or boron,<sup>[3],[4]</sup> can accommodate at the interstitial holes of the Pd host metal system and form analogous structures to that of its interstitial hydrides. With the rapid development in analytical facilities, such as transmission electron microscopy equipped with aberration corrector, and

## COMMUNICATION

diffraction techniques served with high-quality synchrotron and neutron source, have made significant contributions to establish the structure of these doped nanoparticle systems. Crucially, correlating doping, structure, and activity can help to design and synthesise this class of light element doped interstitial Pd catalysts.<sup>[5]</sup>

Similarly, elements (carbon,<sup>[3]</sup> boron and nitrogen) with sufficiently small radii can be placed in the interstitial sites of other transition metal lattice,<sup>[4],[6]</sup> such as cobalt and nickel.<sup>[7],[8]</sup> The feasibility of filling the interstitial site is empirically assessed using basic geometry in Hägg's rule.<sup>[9]</sup> This rule states that the ratio of dopant atomic radius ( $r_X$ ) to that of host metal atomic radius ( $r_M$ ) can be used to guide the structural behaviour after alloying foreign elements. When the ratio ( $r_X/r_M$ ) is less than 0.59, the structure of the 'interstitial' alloy is expected to form. However, there is also an electronic effect that critically affects whether an interstitial atom can be accommodated. In other words, the nature of metallic bonding in interstitial solid-solution transition-metal alloys (d-orbital dominated) significantly differ from the pristine metal because of orbitals mixing between the foreign atoms and the host metal system, for instance, the s-p orbitals of the foreign element and the s-p-d orbitals of the transition metal element can be intermixed. According to the Engel-Brewer theory of metals,<sup>[10]</sup> it was considered that the structure adopted by a metal or interstitial solid-solution alloy is governed by s-p electron configuration.<sup>[11]</sup> Furthermore, the presence of foreign atoms in a metal structure can lead to lattice change of the host structure, which is the key indicative of interstitial solid-solution alloy formation owing to the electrostatic interactions.<sup>[12]</sup> In addition, under a reducing environment, the partial catalytic reduction of interstitial cationic species by the host structure may form neutral or anionic dopant species that are larger, and no longer able to be accommodated at the interstitial site. The delicate balance of these interactions makes it difficult to understand the structure-activity relationships in supported-metal catalyst systems.

We are particularly interested in the structure of Li doped transition metals and their catalytic performance in hydrogenation reactions. General speaking, cationic lithium is theoretically small enough to take residence in the interstitial sites of most transition metal lattices, but neutral lithium atoms are too large. The location of Li and the oxidation state (electronic interaction) with the host transition metal are important. For example, we reported that interstitial lithium doped palladium (Pd-<sup>int</sup>Li NPs) can be synthesised by heating the mixture of Li(OAc)·2H<sub>2</sub>O and Pd/C at elevated temperatures. The Li (nearly metallic) takes residence in structural distorted interstitial sites under hydrogenation conditions, which can completely suppress the formation of the  $\beta$ -hydride phase and avoid over-hydrogenation beyond the target ethylene products.<sup>[13]</sup>

Binary nanoalloys of Pt with other transition metals are well-researched; however, alloying Pt with light s-block elements after extensive reduction are hardly explored. To the best of our knowledge, the only example is reported by Ohsaka et al. that the electro-deposition of Li on a Pt electrode in propylene carbonate can result in the formation of a Pt-Li alloy, which exhibited enhanced activity in the catalytic oxidation of formic acid relative to a pristine Pt electrode.<sup>[14]</sup> However, the characterization of the obtained catalyst lacked structural and electronic detail, crystallographic siting, and chemical form of the lithium. In contrast, the high temperature synthesis of the Pt-Li binary system at the bulk scale can be dated back to the early 20th century. According to the phase diagram of a Pt-Li bulk system, Pt and Li can form four different stoichiometric compounds : LiPt<sub>2</sub>,<sup>[15]</sup> LiPt,<sup>[16]</sup> LiPt<sub>7</sub>,<sup>[17]</sup> and Li<sub>2</sub>Pt.<sup>[16]</sup> Recently, Howies et al.

## COMMUNICATION

reported a novel intermetallic compound  $\text{Li}_{11}\text{Pt}_2$ , which can be obtained under even harsher conditions.<sup>[18]</sup> Notice that these bulk phases are unable to be used as catalysts due to the low surface area, limited concentration of exposed metal sites, and high lithium contents. Therefore, it is highly important to bridge the knowledge gap between these bulk systems and the analogous nanoparticle system by using the controlled Li doping of supported Pt nanoparticles for catalytic applications.

In this work, we have attempted to synthesise Pt-Li NPs according to a previously reported synthetic strategy with limited Li content.<sup>[13]</sup> With the aid of SXRD (synchrotron X-ray diffraction) and the associated refinement, we report that the unit cell of the Pt metal lattice contracts after lithiation whilst retaining the parent FCC structure. This unique physical change is attributed to the substitution of Pt atoms with Li atoms to form an ordered  $\text{Pt}_7\text{Li}$  phase, which is for the first time confirmed by the STEM-ADF image. In addition, further characterization techniques such as X-ray photoelectron spectroscopy (XPS), solid state nuclear magnetic resonance (ssNMR), thermogravimetric analysis (TGA) and transmission electron microscopy (TEM) (see supporting information) were used to support the findings. We highlight that the combination of characterization techniques clearly provides valuable insights into the siting of Li in the Pt metal lattice and the impact on the catalytic hydrogenation of carbonyl compounds, which exhibits a different mechanism to the analogous Pd-Li system.

**XRD**

In this study, the preparation of Pt-Li/C was investigated by adapting our previously published synthetic strategy, which was developed for Pd-Li/C, for which  $^{\text{int}}\text{Li}$  was confirmed by various techniques.<sup>[13]</sup> The pristine Pt/C NPs after thermal treatment were used as the parent framework material. Mixtures of the Pt/C NPs and  $\text{Li}(\text{OAc})\cdot 2\text{H}_2\text{O}$  were annealed at different temperatures. X-ray diffraction (XRD) of pristine Pt and lithiated Pt illustrated the structural changes induced by annealing at different temperatures, namely a contracted unit cell and increasing crystallite size. As depicted in Figure 1, it is shown that the Pt reflections shift to higher angle for samples annealed at 650 °C: (111), 39.88° to 40.50°; (200), 46.42° to 47.06°; (220), 67.56° to 68.57°; (311), 81.33° to 82.53°; (222), 86.20° to 87.08°. According to the Bragg equation, the *d*-spacing corresponding to each diffraction index contracts from  $d_{(111)} = 2.258 \text{ \AA}$  to  $2.224 \text{ \AA}$ ;  $1.954_{(200)}$  to  $1.928_{(200)} \text{ \AA}$ ;  $1.385_{(220)}$  to  $1.367_{(220)} \text{ \AA}$ ;  $1.182_{(311)}$  to  $1.167_{(311)} \text{ \AA}$  and  $1.127_{(222)}$  to  $1.117_{(222)} \text{ \AA}$ , respectively. Obviously, there is a clear contraction of the lattice parameter from  $3.92 \text{ \AA}$  to  $3.89 \text{ \AA}$  (see Table S5). This analysis also suggests that Li species can preferably react with the Pt metal framework at elevated temperatures, which is consistent with the TGA profile. (Supporting information Figure S1 and Table S2)

Additionally, when the temperature reached to the 750 °C, extra peaks were found at the range of 50-70°. The diffraction peaks located at 56.76° and 66.56° are indexed to (220) and (311) of the  $\text{Li}_2\text{O}$  phase.<sup>[19]</sup> Again, the result agrees with the TGA data (Supporting information Figure S1 and Table S2) which showed the decomposition of Li acetate to  $\text{Li}_2\text{O}$  under the reaction condition. The rest of low-intensity peaks could be indexed to (133), (024), (224) and (115) of the  $\text{Pt}_7\text{Li}$ , respectively, on the basis of the literature, but requires for further evidence.<sup>[17]</sup>

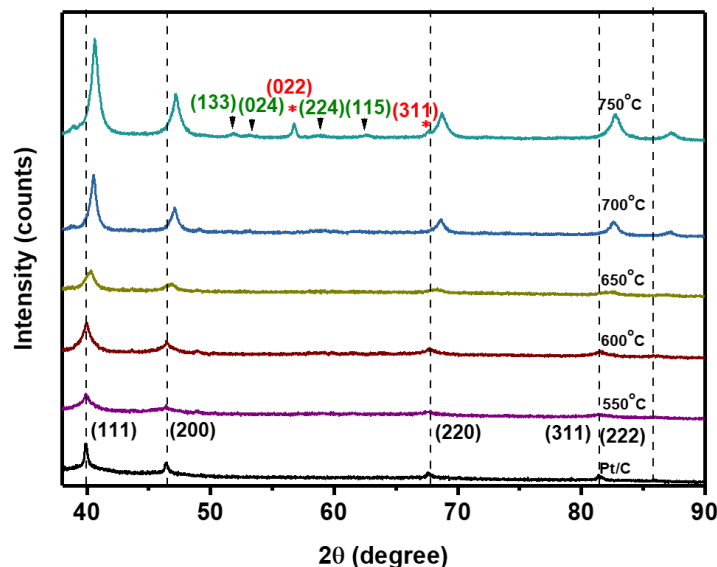


**Figure 1.** XRD patterns of Pt/C with Li(OAc) $\cdot$ 2H $_2$ O after annealing at temperatures between 550 °C and 750 °C for 2 hours. Dotted lines indicate the original positions of Pt diffraction patterns. It can be found that the Pt reflections shift to higher angle when the annealing temperature is above 650 °C. The diffraction peaks of Li $_2$ O are annotated with symbol \*, while the diffraction peaks of Pt $_7$ Li are annotated with symbol ▼.

With the development of high quality X-rays at synchrotrons through improvements in collimation, flux, detection, and energy bandwidth,<sup>[20]</sup> high-resolution diffraction data can be collected. In comparison with the pristine Pt SXRD pattern, the Pt-Li reflections shift to higher angles, which is consistent with our observations using lab-source XRD. Additionally, weak low-angle peaks were detected at the range of 8 to 32°, which were indexed and assigned following more intensive refinement (Figures S5 and S6). Following the simulation of various Pt-Li based compounds, the broad peaks, observed at  $2\theta = 10.5^\circ$ ,  $12.2^\circ$ ,  $17.2^\circ$ ,  $20.2^\circ$ ,  $26.7^\circ$  and  $27.3^\circ$  (Figure S6b), have been well matched to the structure of the known *Fm-3m* intermetallic compound Pt $_7$ Li, which is coincident with the aforementioned observation (Table S5).

### Atomic ADF-STEM using ptychography

The structure of Pt $_7$ Li results from the ordered substitution of Pt atoms with Li. In order to confirm the presence of <sup>sub</sup>Li atoms within the Pt $_7$ Li phase, we then characterized the structure by electron microscope. On the basis of the BF-TEM image and its corresponding histogram (Figure S8a and b), particles are well-dispersed on the carbon support, and 50 NPs were counted. The size distribution is at the range of 2-16 nm.

Aberration-corrected electron microscopy was used to directly visualize the atomic arrangement of a selected Pt-Li NP. Additionally, being a phase imaging technique, electron ptychography is highly sensitive to light elements, such as Li and is therefore applicable to this system.<sup>[21]</sup> We thus simultaneously carried out ADF imaging and ptychography at the atomic level through the use of fast pixelated detectors.

## COMMUNICATION

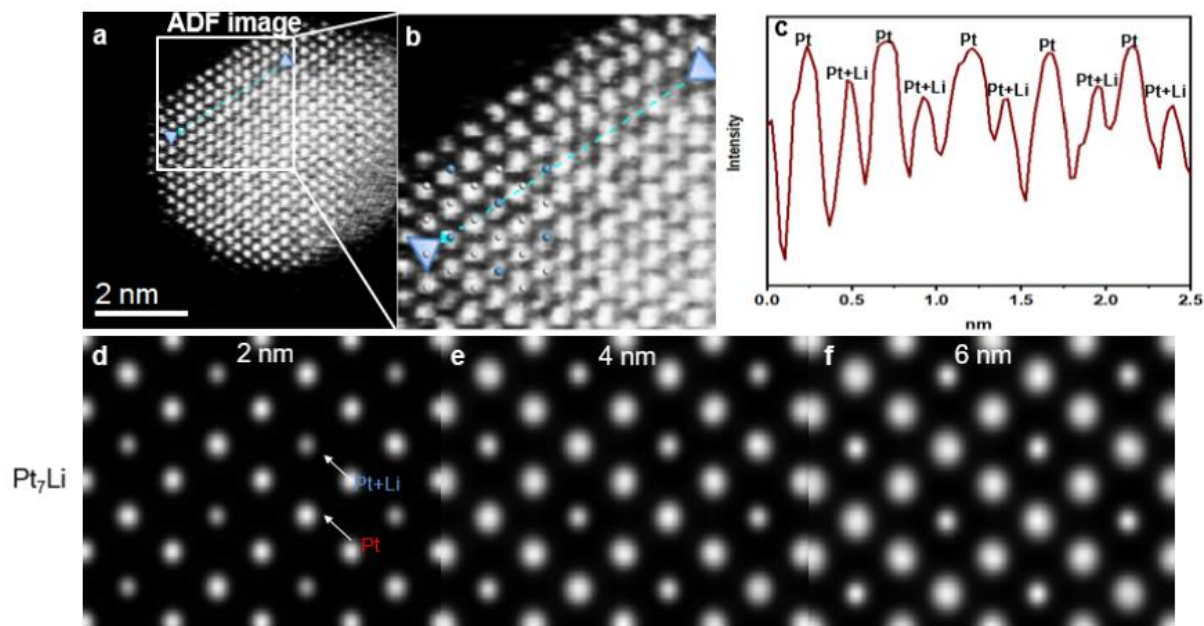


**Figure 2.** Simultaneously acquired Z-contrast STEM-ADF. (a). Z-contrast STEM-ADF micrograph of Pt-Li/C NP orientated in the  $\langle 110 \rangle$  zone axis. (b) Enlarged area of the NP with Pt<sub>7</sub>Li  $\langle 110 \rangle$  model superimposed (blue: mixed Pt and Li, gray: Pt). (c). ADF intensity line profile taken along the line indicated in (a). (d), (e) and (f) are simulated ADF imaging for Pt<sub>7</sub>Li of different thicknesses.

Owing to the strong relationship between atomic number and electron-scattering ability, the intensity of ADF image of an atomic column is highly dependent on the number and element of the atoms being imaged. In this case, lithium atoms are expected to scatter much less than the heavy platinum atoms given the approximately identical number of atoms in each column. Consequently, in a typical Z-contrast STEM-ADF image of Pt-Li/C orientated in the  $\langle 110 \rangle$  direction, alternate columns of exclusively Pt atoms and Pt-Li mixed columns were observed. The stronger scattering of Pt relative to Li (Figure 2a-c) result in significant contrast due to the large difference in electron-scattering ability, and allows their differentiation. The STEM micrograph was compared with the Pt<sub>7</sub>Li structure solution as determined by Rietveld refinement of the SXRD pattern in order to verify the structure of the NP. As the model crystal structure of the Pt<sub>7</sub>Li is superimposed on the micrograph, a very good match was indeed found between this model and the NP structure (Figure 2b). It is shown by the intensity line profile of the ADF image that alternating atomic columns are less bright than others, indicating the presence of lithium at a substitutional site within such columns (Figure 2c). The contrast of the restored phase image (Figure S9 a-c) is indistinguishable to that of the STEM-ADF imaging. Except for this, no unusual contrast was found at the interstitial sites of the Pt metal framework,<sup>[3]</sup> which suggests that Li dopants are not located at the interstitial sites. Meanwhile, a spectroscopic technique, electron energy loss spectroscopy (EELS), was attempted to confirm the presence of Li at local environment and resolve the quantification of Pt : Li, but failed to give an acceptable result (Figure S10).

To confirm the validity of the STEM-ADF result, images of Pt<sub>7</sub>Li of varying thickness was also simulated (Figure 2d-f). These simulated images show that the total integrated intensity of the Pt columns is also much higher than the adjacent Pt columns containing Li atoms (see structure

## COMMUNICATION

and viewing directions of Pt<sub>7</sub>Li in Figure S7a). Thus, this is compelling evidence for lithium occupying framework platinum sites in an ordered manner. The observation also supports the postulation that the shifted reflections discussed above are the substitutional-doped platinum. On the basis of the above results, a reaction mechanism is proposed for the formation of the Pt<sub>7</sub>Li. The thermal decomposition of the Li(OAc)·2H<sub>2</sub>O can give the intermediate Li<sub>2</sub>CO<sub>3</sub> which might further decompose to a finely divided oxide, Li<sub>2</sub>O with increasing temperature.<sup>[22]</sup> Elevated temperature and catalytic phase change can promote this process to accelerate the slow diffusion of ions in the solids, and to overcome the strong Columbic attractions between the ions. Subsequently, Li<sub>2</sub>O could be reduced and exchanged with Pt, in the presence of hydrogen atmosphere at elevated temperature.<sup>[17]</sup> Since the material was prepared via a wet-impregnation method, the source of the hydrogen may come from the ethanol and/or water of the hydrated Li(OAc)·2H<sub>2</sub>O precursor. The principle of categorizing mixed-alloys into intermetallic compounds or solid-solution alloys is dependent on the atomic ordering. In intermetallic compounds, they give both long-range atomic order and well-defined stoichiometry, however, in mix-alloys, two metals are randomly and thoroughly mixed.<sup>[23]</sup> In light of the SXRD refinement result, the Bragg constituent is *Fm-3m* matching with crystalline Pt<sub>7</sub>Li. Hence, in combination with the ADF and solid-state nuclear magnetic resonance (ssNMR) results (Figure S2), it can be concluded that the mixture of the thermal decomposition of Li(OAc)·2H<sub>2</sub>O in the presence of Pt/C NPs can yield a Li-substituted Pt intermetallic nanoalloy (Pt<sup>-sub</sup>Li).

### Catalytic Hydrogenation for HMF

The selective hydrogenation of unconjugated carbonyl compounds to their corresponding alcohols represents an important industrial challenge in catalyst development because cleavage of the facile C-O bond must be prevented in the liquid phase. Doped palladium is known to be one of the most effective heterogeneous catalysts for selective hydrogenation of carbon-carbon double bond in unsaturated aldehydes and ketones. However, such selective reactions are quite problematic when carbonyl groups of the substrate are conjugated to double bonds or to an aromatic ring.<sup>[24]</sup> Here, we used hydroxymethylfurfural (HMF), which is an important chemical derived from biomass. It contains a facile carbonyl group that can be used to investigate partial hydrogenation over our supported Pt<sup>-sub</sup>Li catalyst. The desired product is the partially hydrogenated 2,5 - bis(hydroxymethyl)furan (BHMF) by selective hydrogenation of carbonyl to alcohol. Over-hydrogenation commonly takes place over supported Pt catalysts by hydrogenic activation of the facile carbonyl group to yield 5-methyl-2-furanmethanol (MFA, furfuryl alcohol (FA), or even reacting with IPA to 5-[(1-methylethoxy)methyl]-2-furanmethanol (MEFA). Further hydrogenation or hydrodeoxygenation (HDO) reactions can lead to

2,5-Dimethyltetrahydrofuran (DMTHF) or 2,5-dimethyl furan (DMF), or induce ring-opening yielding side products such as hexane, 2-hexanol, 2-hexanone, etc. (Figure 3).

Thus, the conversion of HMF and the product selectivity of BHMF were carefully analyzed by analyzing quenched aliquots at different times of a batch reaction. The reaction temperature was initially at 100 °C and 120 °C, respectively. The Li content was optimized for selectivity of BHMF, the result of which is summarized in the supporting information (Table S7). The time-course of hydrogenation HMF over Pt/C and Pt<sup>-sub</sup>Li/C (conversion and the selectivity to BHMF) is displayed in Table 1.

## COMMUNICATION

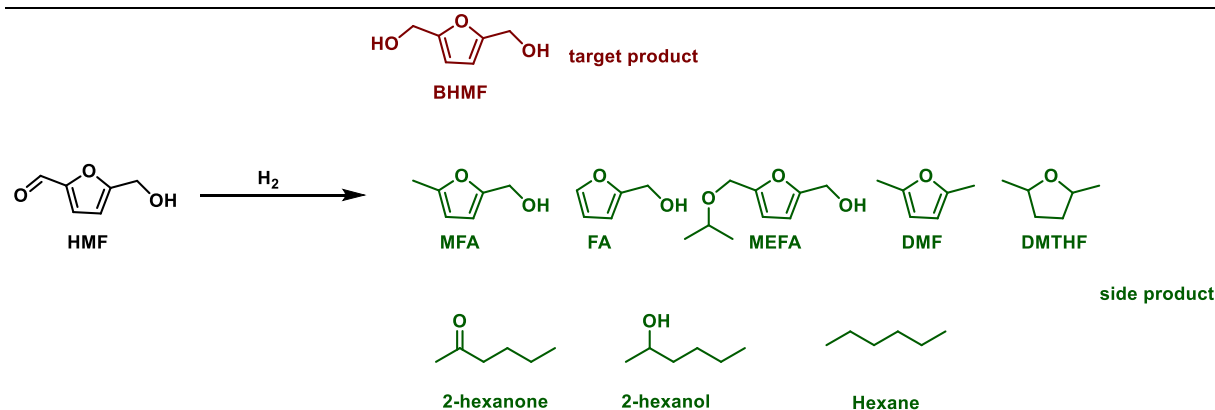


**Figure 3.** Hydrogenation of hydroxyl methyl furan (HMF) to 5-methyl furfuryl alcohol (MFA); furfuryl alcohol (FA); 5-[(1-methylethoxy)methyl]-2-furanmethanol (MEFA); 2,5-Bis(hydroxymethyl)furan (BHMF); 5-methyl furfural (MF) and other side products, etc.

**Table 1.** Time-course regarding the conversion and product selectivity of the selective hydrogenation of HMF over Pt/C and Pt<sup>sub</sup>-Li/C in IPA at 100 °C.

Catalyst	Reaction Time (h)	HMF conversion (%mol)	BHMF Select. (%mol)	MEFA Select. (%mol)	MFA Select. (%mol)	Side products Select. (%)
Pt/C	1	94	11	30	4	55
Pt/C	2	>99	9	32	Trace	59
Pt/C	4	>99	7	18	Trace	75
Pt <sup>sub</sup> -Li/C	1	86	87	1	9	3
Pt <sup>sub</sup> -Li/C	2	98	93	1	6	Trace
Pt <sup>sub</sup> -Li/C	4	99	93	Trace	5	2

At 100 °C, Pt/C exhibited only 11% selectivity towards BHMF, despite a conversion of 94% after one hour. The major side-product was MEFA showing that the excessive adsorption of facile carbonyl group of HMF on unmodified Pt surface can lead to hydrolytic cleavage, in addition to by-products such as liquid alkanes, ring-opening products and intermediate fragments (Figure 3). At higher temperature (120 °C) or longer reaction times, it was found that the BHMF and the carbonyl-cleaved intermediates, such as MEFA and MFA, were substantially decreased at the expense of other further fragmented hydrocarbon products (Table S7). This result clearly indicates poor intrinsic selectivity towards BHMF due to the adsorption of the carbonyl group of the HMF molecule on Pt. In contrast, Pt/C treated with Li(OAc)·2H<sub>2</sub>O (0.5 eq.) results in lower activity with a 86% conversion of HMF after 1 hour, but with a significantly improved selectivity for the partially-hydrogenated product BHMF of 87%. Reaction intermediates, such as furfural and MEFA, were not observed by GC-MS analysis. Prolonging the reaction time to two hours, a near-total conversion of HMF was observed (98-99%), for which the BHMF selectivity increased to 93%. Optimization of temperature (120 °C) and time (2 hours) can give stoichiometric conversion of HMF to BHMF, accompanied by only a trace of other products (Table S7).

In contrast to the unmodified Pt commercial catalyst, the Pt<sup>sub</sup>-Li catalyst exhibits exclusive conversion of HMF to BHMF without cleavage of the facile C-O bond. Instead of blocking the

## COMMUNICATION

interstitial sites from hydrogen accommodation and the resulting excessive hydrogenation, as is the case for the palladium system Pd-<sup>int</sup>Li, the catalytic activity and selectivity of Pt metal NPs may also be altered by the position of the d-band centroid of the metallic structure,  $\epsilon_c$ , and the degree of electron filling with respect to the Fermi level. The downshift of the d-band centroid will decrease the adsorbate-substrate binding strength, whereas the degree of electron filling will also reduce the binding energy.<sup>[25]</sup> Substitutional Li doping results in only a small change in the lattice parameter, hence the effect of d-band down-shifting is weak.<sup>[26]</sup> In addition, lithium is a highly electropositive element that does not have available p or d orbitals for hybridizations with the host framework atoms which alter the Pt d-band position (in contrast to other light element dopants such as boron and carbon). Hence electron filling is anticipated to cause substantially weaker adsorption of the HMF carbonyl, resulting in selective conversion to BHMF, with total inhibition of over-hydrogenated or related products. It is believed that this direct correlation between the doped structure and catalytic hydrogenation activity will allow the development of new catalytic applications.

In conclusion, lithium-doping pre-reduced supported Pt NPs is shown to be substitutional by the formation of a discrete Pt<sub>7</sub>Li crystalline phase, shown by SXRD in the emergent low angle phase and an unusual contraction in the framework Pt lattice parameter. Additionally, analysis of STEM-ADF images directly shows the low-scattering Li atoms to be present in alternating atomic columns, further verifying the observation of substitutional doping. Hence, it can be found that a consequence of the ordered substitution is that the crystal can be conceptualised as alternating layers of only Pt and layers of alternating Pt-Li. To the best of our knowledge, it is the first time Pt-<sup>sub</sup>Li has been synthesized and characterized in the form of a powder nanocatalyst. Their catalytic performance was tested in the hydrogenation of biomass-derived HMF to selectively produce BHMF. We show that the presence of the Li dopant can dramatically suppress the formation of side products by inhibiting the extensive hydrodeoxygenation (HDO) reaction pathways. It is anticipated that the electron filling of the d-band center of the Pt after lithiation without high-order orbital hybridizations can severely weaken the adsorption of HMF molecules, leading to retention of the C-O bond and higher selectivity towards the partially-hydrogenated product, BHMF.

**Experimental Section**

Experimental Details are available in the supporting information.

**Conflicts of interest**

The authors declare no competing financial interest.

**Acknowledgements**

The support of this project from the IUK-EPSRC of UK (DGE 102000) is gratefully acknowledged. The authors wish to thank Diamond Light Source (Diamond, UK) for accessing STEM and XAS facilities (B18; SP20856-1).

**Keywords:**

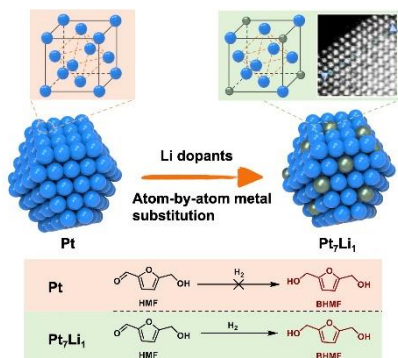
Bimetallic, Substitution, Ordered alloy, Nanoparticle, Hydrogenation



## COMMUNICATION

- [1] G. C. Bond, *Heterogeneous Catalysis: Principles and Applications*, Clarendon Press, Oxford, **1987**, p.10–112.
- [2] F. Z. Haber, *Electrochemistry* **1898**, 22, 506–514.
- [3] Y. Xiao, J.Y. Hwang, Y.K. Sun, *J. Mater. Chem. A* **2016**, 4, 10379–10393.
- [4] S. Carenco, D. Portehault, C. Boissière, N. Mézailles, C. Sanchez, *Chem. Rev.* **2013**, 113, 7981–8065.
- [5] T. Chen, I. Ellis, T. J. N. Hooper, E. Liberti, L. Ye, B. T. W. Lo, C. O’Leary, A. A. Sheader, G. T. Martinez, L. Jones, P. L. Ho, P. Zhao, J. Cookson, P. T. Bishop, P. Chater, J. V. Hanna, P. Nellist, S. C. E. Tsang, *J. Am. Chem. Soc.* **2019**, 141, 19616–19624 .
- [6] A. B. Dongil, *Nanomaterials* **2019**, 9, 1111–1129.
- [7] A. J. Al Abdulghani, J. H. Park, S. M. Kozlov, D. C. Kang, B. AlSabban, S. Pedireddy, A. Aguilar-Tapia, S. Ould-Chikh, J. L. Hazemann, J. M. Basset, L. Cavallo, K. Takanabe, *J. Catal.* **2020**, 392, 126–134.
- [8] Y. Niu, X. Huang, Y. Wang, M. Xu, J. Chen, S. Xu, M. Willinger, W. Zhang, M. Wei, B. Zhang, *Nat. Commun.* **2020**, 11, 3324.
- [9] G.Hägg, *Phys. Chem. B* **1931**, 12, 33.
- [10] S. T. Oyama, *Catal. Today* **1992**, 15, 179–200.
- [11] L. Brewer, *Science*. **1968**, 161, 115–122.
- [12] J. S. Galsin, in *Impurity Scatt. Met. Alloy.*, Springer US, Boston, MA, **2002**, p. 93–123.
- [13] I. T. Ellis, E. H. Wolf, G. Jones, B. Lo, M. Li, A. P. E. York, S. C. Tsang, *Chem. Commun.* **2017**, 53, 601–604.
- [14] Z. Awaludin, T. Okajima, T. Ohsaka, *Electrochem. commun.* **2013**, 31, 100–103.
- [15] C. P. Nash, F. M. Boyden, L. D. Whittig, *J. Am. Chem. Soc.* **1960**, 82, 6203–6204.
- [16] W. Bronger, B. Nacken, K. Ploog, *J. Less Common Met.* **1975**, 43, 143–146.
- [17] W. Bronger, G. Klessen, P. Müller, *J. Less Common Met.* **1985**, 109, L1– L8.
- [18] J. Binns, M. Marqués, P. Dalladay-Simpson, R. Turnbull, M. Frost, E. Gregoryanz, R. T. Howie, *Phys. Rev. B* **2019**, 99, 220101.
- [19] R. W. G. Wyckoff, *Crystal Structures-Volumes I*, Interscience Publishers, New York, **1963**, p.1–339
- [20] B. T. W. Lo, L. Ye, S. C. E. Tsang, *Chem* **2018**, 4, 1778–1808.
- [21] J. G. Lozano, G. T. Martinez, L. Jin, P. D. Nellist, P. G. Bruce, *Nano Lett.* **2018**, 18, 6850–6855.
- [22] L. Shi, T. Qu, D. Liu, Y. Deng, B. Yang, Y. Dai, in *Mater. Process. Fundam. 2020*, Springer, Cham, **2020**, p. 107–116.
- [23] Y. P. Wang, B. S. Li, H. Z. Fu, *Adv. Eng. Mater.* **2009**, 11, 641–644.
- [24] I. V Komarov, V. E. Denisenko, M. Yu.Kornilov, *Tetrahedron* **1994**, 50, 6921–6926.
- [25] T. Chen, C. Foo, S. C. Edman Tsang, *Chem. Sci.* **2021**, 12, 517–532.
- [26] Z. Xia, S. Guo, *Chem. Soc. Rev.* **2019**, 48, 3265–3278.

## COMMUNICATION



It is observed for the first time a direct 'substitution' of Pt with <sup>sub</sup>Li in atomic columns by electron ptychography images with characteristic contraction in lattice parameters from advanced materials characterization. The electron donation of d-band of Pt without higher orbital hybridizations by <sup>sub</sup>Li offers an alternative way for ultra-selectivity in catalytic hydrogenation of carbonyl compounds with detainment of facile CO bond to alcohols.